Pergamon

Int. J. Heat Mass Transfer. Vol. 39, No. 7, pp. 1535–1542, 1996

0017-9310/96 $15.00+0.00

0017-9310(95)00231-6

Irreversibility analysis of a sieve tray in a distillation column

S. RAY and S. P. SENGUPTA

CAPE Laboratory, Department of Chemical Engineering, Indian Institute of Technology Kharagpur, 721 302, India

(*Received* 28 *September* 1993 *and in final form* 16 *March* 1994)

Abstract—A Second Law analysis has been developed for a vapor–liquid contacting device as in the sieve tray of a distillation column. Using a discrete bubble dynamics model, an equation for entropy balance has been formulated to numerically evaluate the entropy generation rate associated with heat, mass and momentum transfer for bubble movement through a moving liquid pool. The entropy generation rates per unit bubble mass have been evaluated for variations in sieve tray parameters like orifice diameter and weir height for fixed separation characteristics of components constituting the two phases. It has been found that among the tray parameters, weir height plays a dominant role compared to sieve hole diameter on entropy generation.

INTRODUCTION

The Second Law Analysis of any process attempts to evaluate the entropy generation rate as a function of pertinent input parameters. Estimation of process irreversibilities from entropy generation rate and minimization of the same through suitable adjustments of the process variables is referred to as the thermodynamic optimization of the process. This analysis is of prime importance from the practical aspect of efficient use of energy resources. Available energy loss in any process should be kept to a minimum, meeting the consideration of other physical constraints which are used to achieve the overall economy of the process. Among all separation processes in the Chemical Process Industry, distillation has the maximum share of energy input [1] and hence merits a special focus for any possible improvement in energy utilization. Sieve trays are used in distillation columns for intimate vapor liquid contact.

Studies on entropy generation rates for convective heat transfer problems in general were extensively reported by Bejan [2, 3]. Among the related work involving internal flow through simple ducts and typical heat exchangers, mention can be made of Bejan [4, 5], Golem [6], Sarangi [7] and Nag [8]. A Second Law analysis of spray evaporation has also been reported by Som [9].

Entropy generation effects are associated with simultaneous heat, mass and momentum transfer on the trays. The fundamental process on the tray is formation of vapor bubbles and their interaction with the liquid flowing across the tray. Energy is also dissipated due to friction of the liquid with the tray internals.

The studies on irreversibility and their interaction with the transport process in the case of bubble movement on a tray with liquid flowing across the tray is important in determining the total loss in available energy of a separation process involving distillation. No such approach towards an irreversibility analysis of the process of distillation on trays is available in literature to decide the conditions best suited for the process. The present work is an attempt in this direction to numerically evaluate the entropy generation histories in the sieve trays of a distillation column based on the fundamental process on a tray, i.e. formation of vapor bubbles and their interaction with the liquid flowing across the tray. Energy is also dissipated due to friction of liquid with the tray internals.

A large volume of work has been reported in literature [10–15] on bubble formation at a single orifice. All of these deal with isothermal system without any mass transfer and are aimed at predicting bubble size and velocity. The basic approach in the literature reported varies in considerations of orifice upstream pressure variations and other details of modeling.

Entropy generation is a path function and hence the best estimate of entropy generation must be based on a model of the process describing the thermodynamic path of changes as closely and correctly as possible. The proposed model incorporates effects of cross flowing liquid and simultaneous momentum, heat and mass transfer across bubble–liquid interface. Entropy generation in each step has been estimated from the first principles and then integrated for the entire process.

THEORETICAL ANALYSIS

The irreversibility analysis for the process of separation on a single sieve tray as encountered in distillation requires information on heat, mass and momentum transfer during: (i) bubble formation and

NOMENCLATURE

$a, \dot{a}$ bubble radius [m], time derivative of bubble radius
a_o orifice radius [m]
A active area of tray per orifice [m^2]
A_b surface area of bubble [m^2]
A_o orifice area [m^2]
C_o orifice discharge coefficient (≈ 0.61)
c_{pl}, c_{pb}, c_{po} specific heat of liquid, bubble, vapor upstream of sieve tray
h bubble–liquid heat transfer coefficient [J K^{-1}m^{-2} s]
h_w liquid depth on tray (nearly equal to the tray exit weir height) [m]
k_{m_l} liquid phase bubble–liquid mass transfer coefficient
k_{th_l} thermal conductivity of liquid
m_{bf} final mass of the bubble [kg]
Mw_b, Mw_o, Mw_l molecular weight of bubble, molecular weight of vapor upstream of sieve tray, molecular weight of liquid on sieve tray
n_b no. of moles in the bubble
Nu Nusselt number
p_b pressure inside bubble [Pa]
p_l pressure on top surface of liquid [Pa]
ΔP_σ bubble pressure due to surface tension [Pa]
p_{fh}, p_{fv} bubble pressure due to horizontal and vertical components of viscous drag on bubble [Pa]
Pr Prandtl number
R Gas constant [J K^{-1} kg^{-1} mole^{-1}]
Re Reynolds number
s height of the bubble (center of the sphere or part of sphere) above the tray [m]
Sc Schmidt number
Sh Sherwood number
t time [s]
T_l, T_b, T_{bo} temperature (absolute) of liquid, bubble and vapor upstream of sieve tray [K]
u_l, u_s velocity of liquid on tray, slip velocity of bubble [m s^{-1}]
$v, \dot{v}, \ddot{v}$ bubble volume [m^3] and their time derivatives
x, y, y^*, x^* mole fraction of component l in liquid, inside bubble, vapor in equilibrium with x, liquid in equilibrium with x
z horizontal drift of bubble (sphere center) [m]
ρ_l, ρ_b, ρ_o liquid and bubble density [kg m^{-3}], density of vapor upstream of sieve tray [kg m^{-3}]
σ surface tension of liquid [J m^{-2}].

growth up to detachment and (ii) bubble motion through a pool of liquid till rupture on the liquid surface.

The treatment of bubble dynamics prediction for constant pressure bubble formation by La Nauze and Harris [13] is considered most appropriate. Additional assumptions on which further relationships are developed, are:

(1) the system is bi-component;
(2) the mass transfer across the bubble–liquid boundary is equimolal counterflow;
(3) the bubbles are small and are therefore well mixed;
(4) no bubble collapse or coalescence is considered on the tray;
(5) the mass transfer is liquid phase controlling [16].

The process of bubble formation, detachment and movement are shown in Fig. 1. The condition of bubble detachment is $s = a + a_o$.

Momentum transfer

Bubble growth. The bubble grows when the pressure inside the bubble (p_b) exceeds the resisting effects of (a) liquid surface tension, (b) static pressure and (c) drag on the bubble due to relative motion between bubble and liquid. Bubble growth imparts momentum to the surrounding liquid and also imparts vertical acceleration to the liquid column in the tray. The second effect is neglected on a tray as the liquid height is assumed to remain constant due to the overflow over the exit weir of the tray. A pressure balance yields:

$$p_b - \{p_l + \rho_l \cdot g \cdot (h_w - s) + p_o + p_{fh} + p_{fv}\} = \rho_l \cdot h_w \cdot \ddot{v}/A + \rho_l[a \cdot \ddot{a} + 1.5 \cdot (\dot{a})^2]. \quad (1)$$

The Δp_σ term is given by,

$$\Delta p_\sigma = 2\sigma(3a+s)/(3a^2 + 2a \cdot s - s^2), \quad \text{when } s \leqslant a$$

and

$$\Delta p_\sigma = 2\sigma/a, \quad \text{when } s > a. \quad (2)$$

Till the point of detachment, the vapor flows to the bubble under the pressure differential of the orifice upstream and inside of the bubble. The mass flow rate is governed by the conventional orifice equation as,

$$\dot{m}_o = \rho_o \cdot \mathrm{d}(Mw_b \cdot n_b)/\mathrm{d}t = A_o \cdot C_o \cdot [2 \cdot \rho_o \cdot (p_o - p_b)^{1/2}/\{1 - (A_o/A)^2\}]. \quad (3)$$

The volume of bubble and its derivatives from La Nauze and Harris [13] are:

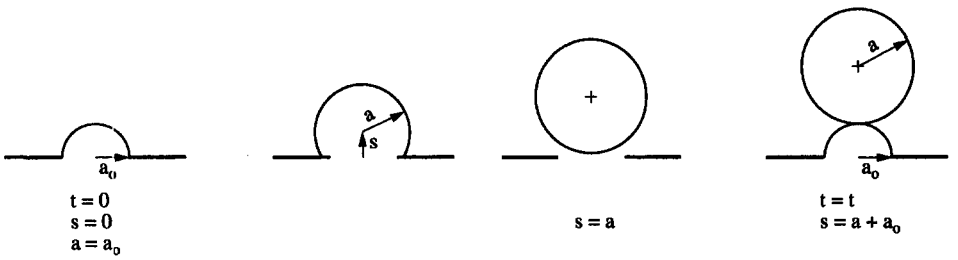

Fig. 1. The bubble formation sequence.

when $s < a$

$$v = \pi(2/3 \cdot a^3 + a^2 \cdot s - s^3/3)$$

$$\dot{v} = \pi(2a^2 \cdot \dot{a} + 2a \cdot \dot{a} \cdot s + a^2 \cdot \dot{s} - s^2 \cdot \dot{s})$$

$$\ddot{v} = \pi[\ddot{a}(2a^2 + 2a \cdot s) + 2\dot{a}^2(2a + 2s) + 4a \cdot \dot{a} \cdot \dot{s} - 2s \cdot \dot{s}^2 + \ddot{s}(a^2 - s^2)]$$

when $s \geqslant a$

$$v = 4\pi/3 \cdot a^3$$

$$\dot{v} = 4\pi a^2 \cdot \dot{a}$$

$$\ddot{v} = 4\pi(2a \cdot \dot{a}^2 + a^2 \cdot \ddot{a}). \quad (4)$$

Bubble motion. The horizontal force on the bubble is due to the horizontal slip velocity $(u_l - dz/dt)$ between the bubble and the flowing liquid on the tray. The resulting equation of motion is,

$$\frac{d}{dt}(n_b \cdot Mw_b \cdot dz/dt) = 0.5C_d \cdot A_h \cdot \rho_l \cdot (u_l - dz/dt)^2 \quad (5)$$

where, A_h is the cross-section of bubble perpendicular to flow direction.

$$A_h = \pi a^2 - a^2 \cdot \tan^{-1}(a_o/s) - a_o \cdot s, \quad \text{when } s \leqslant a$$

and,

$$A_h = \pi a^2, \quad \text{when } s > a.$$

The corresponding equation of motion in vertical direction is therefore,

$$\frac{d}{dt}(n_b \cdot Mw_b\, ds/dt) = v(\rho_l - \rho_b)g - 0.5C_d \cdot \pi \cdot a^2 \cdot \rho_l \cdot (ds/dt)^2. \quad (6)$$

Drag coefficient C_d depends on the bubble Reynolds number $(Re = 2 \cdot a \cdot u_s \cdot \rho_l/\mu_l)$, based on the slip velocity,

where slip velocity,

$$u_s = [(u - dz/dt)^2 + (ds/dt)^2]^{0.5}$$

and the drag coefficient,

$$C_d = 24/Re \quad \text{when } Re \leqslant 1,$$

$$C_d = 18.5/Re^{0.6} \quad \text{when } 1 < Re \leqslant 500$$

$$C_d = 0.44 \quad \text{when } Re > 500.$$

Equivalent pressure terms are obtained as,

$$p_{fh} = 0.5C_d \cdot \rho_l \cdot (u_l - dz/dt)^2$$

and

$$p_{fv} = v(\rho_l - \rho_b) \cdot g/a^2 - 0.5 \cdot a^2 \cdot \rho_l \cdot (ds/dt)^2. \quad (7)$$

Heat transfer

Thermal energy balance. Rate of energy accumulation in the bubble is the difference between the inflow through the orifice along with vapor and the outflow through the bubble–liquid interface. The energy balance equation is,

$$\frac{d}{dt}(n_b Mw_b \cdot c_{pb} \cdot T_b) = Mw_o \cdot (dn_b/dt) \cdot c_{po} \cdot (T_o - T_b) - h \cdot A_b \cdot (T_b - T_l). \quad (8)$$

After bubble detachment, the term dn_b/dt becomes zero.

Mass transfer

Component balance. If the lighter component is denoted as component 1, the accumulation rate of component is the difference between the orifice inflow and the bubble–liquid interface exchange rate. The balance therefore yields,

$$\frac{d}{dt}(n_b \cdot y) = (dn_b/dt) \cdot (y_o - y) - k_{m\_l} \cdot (x - x^*) \cdot A_b \cdot \rho_l/Mw_l. \quad (9)$$

Transport properties in the liquid phase fixes the Sc $(= \mu_l/\rho_l \cdot D_{AB})$ and Pr $(= c_{pl} \cdot \mu_l/k_{th\_l})$ values. Corresponding to these values of Pr, Sc and instantaneous value of Re, the values of h and k_{m_l} values are calculated through $Nu\,(= h \cdot 2a/k_{th\_l})$ and $Sh\,(= k_{m\_l} \cdot 2a/D_{AB\_l})$ expressions [17] given below:

$$Sh = 2. + 0.60 \cdot Re^{0.5} \cdot Sc^{1/3}$$

$$Nu = 2. + 0.60 \cdot Re^{0.5} \cdot Pr^{1/3}. \quad (10)$$

The instantaneous values of the Mw_b, c_{pb}, o_b are estimated from the molecular weight, specific heat of components and bubble composition.

Simultaneous solution of equations (1)–(10) with initial conditions of $a = a_o$, $v = (2\pi/3)a_o^3$, $s = 0$,

$a = 0$, $\dot{a} = 0$, $\dot{s} = 0$ and $dz/dt = 0$ [when $s < (a+a_o)$], gives the variations of bubble volume, velocity, location, temperature and composition with time.

Entropy generation

The entropy generation rate at each instant is contributed by:

$$sg1 = (dn_b/dt) \cdot R \cdot \ln(p_o/p_b) \quad \text{when } s \leqslant (a+a_o)$$

$$sg1 = 0, \quad \text{when } s > (a+a_o) \tag{11}$$

bubble–liquid heat transfer:

$$sg2 = h \cdot A_b \cdot (1/T_l - 1/T_b) \cdot (T_b - T_l) \tag{12}$$

bubble–liquid mass transfer:

$$sg3 = k_{m\_l} \cdot A_b \cdot (x - x^*) \cdot (\rho_l/Mw_l) \cdot \ln[\{y^*(1-y)\}/\{y(1-y^*)\}] \tag{13}$$

dissipation of momentum transferred to surrounding liquid due to bubble expansion:

$$sg4 = \rho_l \cdot (a \cdot \dot{a} + 1.5 \cdot \dot{a}^2) \cdot v/T_l \tag{14}$$

viscous drag on bubble:

$$sg5 = 0.5 \cdot C_d \cdot \pi a^2 \cdot u_s^2 \cdot u_s/T_l \tag{15}$$

work done against static pressure:

$$sg6 = \{p_l + (h-s) \cdot \rho_l \cdot g\} \cdot \dot{v} \cdot /T_l \tag{16}$$

work done against surface tension force:

$$sg7 = \Delta p_\sigma \cdot \dot{v}/T_l. \tag{17}$$

Entropy generation due to bubble bursting. The bubble bursts when the center of the bubble is at a height of $(h_w - a)$ from the tray. The surface tension energy is dissipated as the bubble bursts. The entropy generation due to bubble bursting is,

$$sg8 = \sigma \cdot A_b/(T_l \cdot m_{bf}). \tag{18}$$

Entropy generation per unit mass of vapor bubble is,

$$sb = (1/m_{bf}) \cdot \int_o^{t_f} (sg1 + sg2 + sg3 + sg4 + sg5 + sg6 + sg7) \cdot dt + sg8. \tag{19}$$

At each time instant the entropy generation rates are calculated based on equations (11)–(17), the entropy generation due to bubble bursting is calculated from equation (18), and the total entropy generation per unit mass of bubble (up to and including bubble bursting) is calculated from equation (19).

RESULTS AND DISCUSSION

The theoretical analysis presented, pertains to behavior of a single bubble on the tray and entropy generation estimation based on the bubble–liquid interactions on the tray.

As a case study, a typical distillation sieve tray in a benzene–toluene separation column operating near atmospheric pressure is considered where the pressure drop across the tray is around 0.05 m water column.

	Vapor	Liquid
Temperature [K]	361.2	3599.34
Composition (mole % benzene)	80.097	73.2953

Average cross flow velocity of liquid = 0.032 m s^{-1}

Bubble dynamics

Using the theoretical analysis developed, histories of bubble growth, bubble rise, bubble drift, bubble temperature and bubble composition are predicted for a bubble on the tray. These results are shown in Figs. 2–6. The bubble history can clearly be split into the pre-detachment and post-detachment periods.

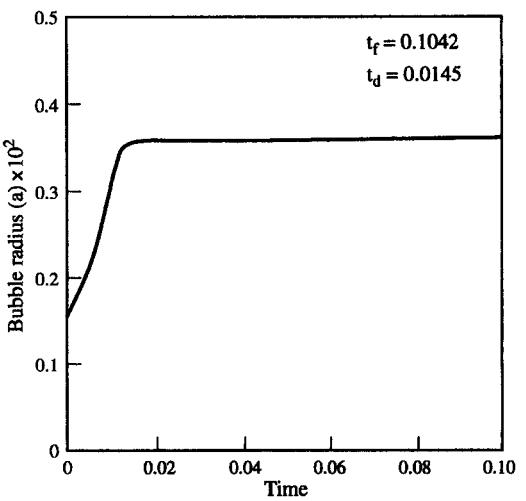

Fig. 2. Growth of bubble radius (a) with time.

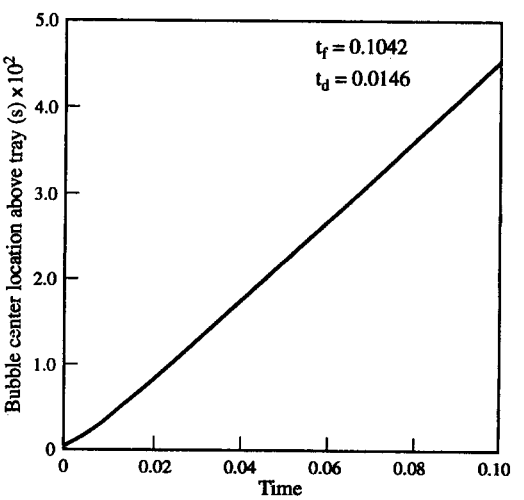

Fig. 3. Rise of bubble (s) with time.

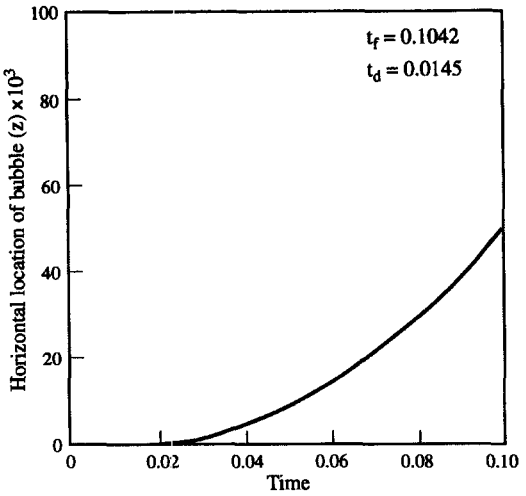

Fig. 4. Horizontal drift (z) of bubble with time.

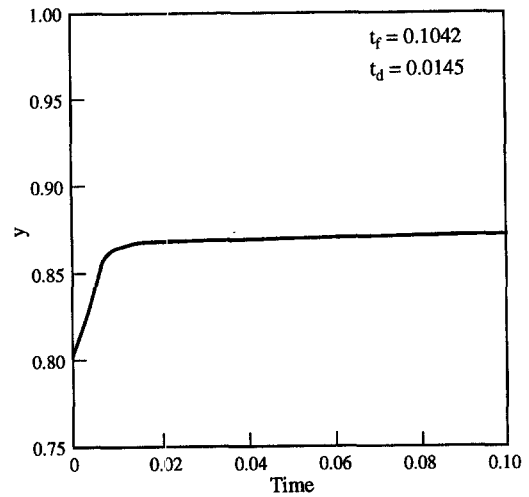

Fig. 5. Bubble composition (y) variation with time.

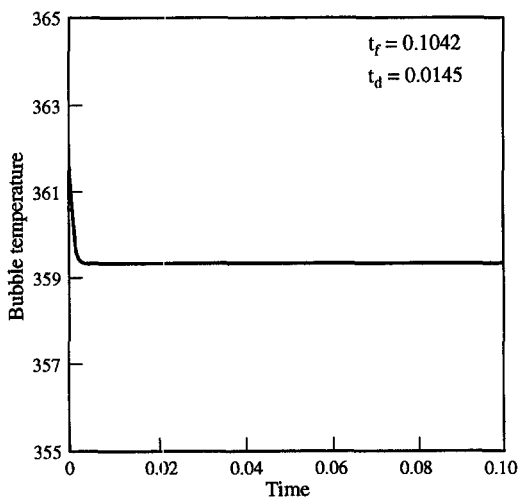

Fig. 6. Bubble temperature (T_b) variation with time.

Bubble growth. The growth of bubble radius with time, shown in Fig. 2, is maximum up to detachment, contributed mainly by the orifice upstream pressure. Beyond detachment, the increase is due to fall in the surrounding static pressure as the bubble rises. The liquid depth on the tray being small, the reduction in surrounding pressure is not very appreciable and the bubble growth beyond detachment is quite small. The bubble average size (bubble radius) from formation to end is 0.0034 m, approximately 2.25 times the orifice diameter. This matches the industrial practices of adopting the pitch for sieve tray holes around two and a half to three times the hole diameter for similar hydrocarbon services. To check further, a nitrogen–oxygen tray with 0.0008 m diameter sieve holes in an air separation column was also studied. This result showed a bubble diameter of 0.0052 m. This is in agreement with the practice of having a pitch of 7–8 times the diameter for the sieve trays in air separation column trays using typically 0.0008 m diameter holes.

Bubble rise. In line with La Nauze [13], the model assumes the bubble to grow from a hemisphere to a complete sphere. Assuming the bubble dimensions to be small, the bubble velocity is taken as the velocity of the center of the sphere (or the truncated sphere in the initial stage of formation of the bubble). Average velocity of the bubble on the tray, as predicted by the model is 0.4798 m s^{-1}. Rise of the bubble with time for the case considered is shown in Fig. 3.

Bubble drift. This is due to the drag of the flowing liquid on the bubble. The result from the model shows that for a liquid velocity of 0.05 m s^{-1}, the final horizontal (drift) velocity attained by the bubble is around 0.011 m s^{-1}. However, the flight time being small, the total drift of the bubble is only of the order of 0.0005 m. Horizontal drift of the bubble with time for the case considered is shown in Fig. 4.

Composition change. The bubble composition (mole fraction of benzene) is found to change from initial value of upstream vapor composition to the final value of concentration (in equilibrium with the local liquid) and is presented in Fig. 5. Most of the concentration change takes place before bubble detachment. High mass transfer coefficient around the growing bubble and high initial driving force of concentration difference are the reasons of this quick change in bubble composition. The bubble leaving the liquid pool has concentration in equilibrium with the surrounding liquid. This corresponds to 100% local efficiency for the system. A low tray efficiency in some practical cases will be due to inadequate vapor–liquid contact like jet flooding on trays, or on account of liquid carry over with vapor.

Temperature change. Similar to the composition change, the bubble temperature change is also almost complete by the time the bubble detaches from the orifice. Probable reasons for this are similar to those already presented in the preceding paragraph. Change in bubble temperature with time is shown in Fig. 6.

Entropy generation

The expressions of entropy generation rate on a tray due to bubble–liquid interactions are developed as entropy generation per unit bubble mass in the section on theoretical analysis. To reduce irreversibility on the trays, the effect of tray design parameters namely, sieve hole diameter, weir height and liquid cross flow velocity are studied. The variation ranges are taken within the limits of practice for the type of tray and service under investigation. Effects of variation of sieve hole diameter and weir height are presented in Tables 1 and 2. Some general observations from these tables are:

Before detachment. Approximately 55% of the total irreversibility is contributed by the phenomena before bubble detachment. During this phase the major contributors are expansion of the bubble and mass transfer.

Beyond bubble detachment. The main contribution comes from viscous drag on bubble and momentum imparted to the surrounding liquid.

Overall. Mass transfer is the largest contributor to irreversibility and accounts for around 30% of the total. Frictional drag on the bubble and work done in bubble growth against liquid contributes around 24% and 42% respectively. Work done during bubble growth against surface tension, bubble bursting, orifice flow and heat transfer contributes the rest of irreversibility. The contribution of bubble–liquid heat transfer to the irreversibility on the tray is rather small.

Table 1. Effect of variation of a_o on entropy generation on tray ($u_l = 0.05$ m s^{-1}, $h_w = 0.050$ m, $x_l = 73.295$ mole %, $y_o = 80.097$, $y^* = 87.050$ mole %)

a_o [m]	0.00150	0.00200	0.00300	0.00400
Bubble life time [s]	0.10420	0.09329	0.08045	0.07236
Detachment time [s]	0.01456	0.01629	0.01895	0.02105
Bubble radius [m]	0.00359	0.00438	0.00567	0.00676
Vertical velocity [m s^{-1}]	0.46103	0.50976	0.58006	0.63327
Drift velocity [m s^{-1}]	0.01146	0.00865	0.00572	0.00415
Bubble drift [m]	0.05594	0.03548	0.01833	0.01096
Entropy generation per unit mass of bubble [J K^{-1} s^{-1} kg^{-1}]—upto bubble bursting				
Due to:				
orifice flow loss	0.02541	0.02022	0.01196	0.00727
bubble–liquid heat transfer	0.00157	0.00179	0.00226	0.00277
bubble–liquid mass transfer	0.42697	0.44366	0.46894	0.49480
viscous drag on bubble	0.35448	0.34175	0.32130	0.30494
dissipation as liquid momentum	0.30193	0.38490	0.44869	0.42640
work against static head	0.31958	0.30723	0.28074	0.25433
work against surface tension	0.01783	0.01412	0.01005	0.00772
bubble bursting	0.02496	0.02043	0.01577	0.01323
Total	1.47273	1.53410	1.55971	2.51146
Entropy generation per unit mass of bubble [J K^{-1} s^{-1} kg^{-1}]—upto bubble detachment				
orifice flow loss	0.02541	0.02022	0.01196	0.00727
bubble–liquid heat transfer	0.00156	0.00177	0.00224	0.00276
bubble–liquid mass transfer	0.40436	0.41914	0.44343	0.47034
viscous drag on bubble	0.01602	0.02056	0.02963	0.03934
dissipation as liquid momentum	0.03217	0.03994	0.04947	0.05316
work against static head	0.31884	0.30649	0.28002	0.25362
work against surface tension	0.01775	0.01406	0.01002	0.00769
Total	0.81611	0.82218	0.82677	0.83418
Entropy generation per unit mass of bubble [J K^{-1} s^{-1} kg^{-1}]—beyond bubble detachment				
bubble–liquid heat transfer	0.00001	0.00002	0.00002	0.00001
bubble–liquid mass transfer	0.02261	0.02452	0.02551	0.02446
viscous drag on bubble	0.33846	0.32119	0.29167	0.26560
dissipation as liquid momentum	0.26976	0.34496	0.39922	0.37324
work against static head	0.00074	0.00074	0.00072	0.00071
work against surface tension	0.00008	0.00006	0.00003	0.00003
bubble bursting	0.02496	0.02043	0.01577	0.01323
Total	0.65662	0.71192	0.73294	1.67728
% Entropy generation per unit mass of bubble upto bubble bursting				
orfice flow loss	1.725	1.318	10.767	0.481
bubble–liquid heat transfer	0.107	0.117	0.145	0.183
bubble–liquid mass transfer	28.991	28.919	30.066	32.737
viscous drag on bubble	24.070	22.277	20.600	20.176
dissipation as liquid momentum	20.501	25.090	28.768	28.212
work against static head	21.700	20.027	17.999	16.826
work against surface tension	1.211	0.920	0.644	0.510
bubble bursting	1.695	1.332	1.011	0.875
Total	100.00 %	100.00 %	100.00 %	100.00 %

Table 2. Effect of variation of h_w on entropy generation on tray ($u_l = 0.05$ m s^{-1}, $a_o = 0.0015$ m, $x_l = 73.295$ mole %, $y_o = 80.097$, $y^* = 87.050$ mole %)

h_w [m]	0.05000	0.06000	0.07000	0.07500
Bubble life time [s]	0.10420	0.12592	0.14768	0.15855
Detachment time [s]	0.01456	0.01456	0.01455	0.01455
Bubble radius [m]	0.00359	0.00359	0.00358	0.00358
Vertical velocity [m s^{-1}]	0.46103	0.46112	0.46111	0.46099
Drift velocity [m s^{-1}]	0.01146	0.01352	0.01533	0.01620
Bubble drift [m]	0.00056	0.00083	0.00115	0.00132
Entropy generation per unit mass of bubble [J K^{-1} s^{-1} kg^{-1}]—upto bubble bursting				
Due to:				
orifice flow loss	0.02541	0.02533	0.02521	0.02517
bubble–liquid heat transfer	0.00157	0.00157	0.00157	0.00158
bubble–liquid mass transfer	0.42697	0.42705	0.42713	0.42735
viscous drag on bubble	0.35448	0.43614	0.51774	0.55849
dissipation as liquid momentum	0.30193	0.36891	0.43791	0.47224
work against static head	0.31958	0.38798	0.45633	0.49060
work against surface tension	0.01783	0.01780	0.01783	0.01781
bubble bursting	0.02496	0.02493	0.02498	0.02496
Total	1.47273	1.68971	1.90870	2.01820
Entropy generation per unit mass of bubble [J K^{-1} s^{-1} kg^{-1}]—upto bubble detachment				
orifice flow loss	0.02541	0.02533	0.02521	0.02517
bubble–liquid heat transfer	0.00156	0.00156	0.00156	0.00156
bubble–liquid mass transfer	0.40436	0.40442	0.40447	0.40468
viscous drag on bubble	0.01602	0.01601	0.01598	0.01597
dissipation as liquid momentum	0.03217	0.03219	0.03224	0.03226
work against static head	0.31884	0.38697	0.45487	0.48897
work against surface tension	0.01775	0.01774	0.01774	0.01774
Total	0.81611	0.88422	0.95207	0.98635
Entropy generation per unit mass of bubble [J K^{-1} s^{-1} kg^{-1}]—beyond bubble detachment				
bubble–liquid heat transfer	0.00001	0.00001	0.00001	0.00002
bubble–liquid mass transfer	0.02261	0.02263	0.02266	0.02267
viscous drag on bubble	0.33846	0.42013	0.50176	0.54252
dissipation as liquid momentum	0.26976	0.33672	0.40567	0.43998
work against static head	0.00074	0.00101	0.00146	0.00163
work against surface tension	0.00008	0.00006	0.00009	0.00007
bubble bursting	0.02496	0.02493	0.02498	0.02496
Total	0.65662	0.80549	0.95663	1.03185
% Entropy generation per unit mass of bubble upto bubble bursting				
orfice flow loss	1.725	1.499	1.321	1.247
bubble–liquid heat transfer	0.105	0.093	0.082	0.078
bubble–liquid mass transfer	28.993	25.274	22.378	21.175
viscous drag on bubble	24.070	25.812	27.125	27.673
dissipation as liquid momentum	20.501	21.833	22.943	23.399
liq col	0.356	0.456	0.559	0.610
work against static head	21.700	22.961	23.908	24.309
work against surface tension	1.211	1.053	0.934	0.882
bubble bursting	1.695	1.475	1.309	1.237
Total	100.00 %	100.00 %	100.00 %	100.00 %

From Table 1, it is seen that opting for a larger sieve hole diameter increases entropy generation. This is due to a faster rate of change from the initial thermodynamic state to the final state as the life time of the bubble is lower with bigger holes. The increase is mainly beyond the phenomena of bubble detachment and is contributed mostly by the momentum transferred to the surrounding liquid. Further it is observed that the entropy generation exhibits a maxima, recommending selection of sieve hole diameter below and above a specific value. This is due to decreasing trend of a as against the increasing trend of a for increasing sieve hole diameters.

Increasing weir height increases irreversibility mainly due to increased work done against the static head. This is shown in Table 2. This increase is during bubble growth, most of which is before bubble detachment. Beyond detachment, the increase is primarily due to higher viscous drag on bubble and momentum imparted to the surrounding liquid.

Higher liquid cross flow velocity on the tray within the practical range increases irreversibility only by a small amount and is therefore not tabled separately. The main cause of increase is higher frictional dissipation between the bubble and liquid.

Apart from the bubble–liquid interactions on the tray leading to entropy generation, the other contribution to entropy generation on a tray comes from

the frictional dissipation due to liquid flowing across the tray internals and through the downcomer. This dissipation is included in the downcomer back-up.

The case of the tray under investigation belongs to a distillation column with 8 $m^3 h^{-1}$ feed of 50 mole % benzene and 50 mole % toluene, being separated to top and bottom products of 95% and 5% benzene, respectively. The tray diameter is 0.75 m and the liquid and vapor rates are 2441.4 kg h^{-1} (0.841 l s^{-1}) and 3513.5 kg h^{-1} (91254.3 l s^{-1}) respectively. At the conditions of the tray, the entropy generation due to vapor–liquid interactions alone amounts to 1.47273 J K^{-1} kg^{-1} of vapor, i.e. 1.44 J K^{-1} s^{-1} for the tray under consideration. A downcomer back-up of 0.30 m is estimated with the operating conditions of the tray. Corresponding to this pressure drop, the entropy generation rate is 0.0055 J K^{-1} s^{-1}. This quantity is negligible in comparison to the contribution of the bubble–liquid interactions on the tray.

CONCLUSIONS

Conclusions that could be drawn from the study are:

(1) The major contributor to irreversibility on a sieve tray in a distillation column for separation of light hydrocarbons is the bubble–liquid interaction on the tray. The effect of interaction of the flowing liquid with the tray internals is negligible. To elaborate:

(a) mass transfer is the largest contributor to irreversibility on a tray. Significant contribution also is from drag on bubble and work done against liquid during bubble growth. The contribution from heat transfer is found to be small.

(b) For the bubbles forming at the sieve tray holes, most of entropy generation is before the bubble detachment. Mass transfer and work done against liquid during bubble growth are the major causes of entropy generation at this stage. Beyond detachment, the main contribution to entropy generation comes from viscous drag on bubble.

(c) For systems of light hydrocarbons with sieve trays, the local tray efficiency is expected to be high, as most of heat and mass transfer occurs before bubble detachment.

(d) Predictions of bubble diameter using the analysis developed for bubble formation with simultaneous heat, mass and momentum transfer agree well with the practices of selecting sieve tray hole pitch. The model also predicts the bubble growth beyond detachment to be small.

(2) Selection of tray design parameters like weir height and sieve hole diameters influences entropy generation. Further:

(a) the effect of weir height is dominant compared to the effect of sieve hole diameter.

(b) A lower sieve hole diameter and a lower weir height is preferred, subject to the constraints of flooding, dumping, etc. which may lead to poorer vapor–liquid contacting.

(c) whereas the increasing weir height shows a monotonic increase in entropy generation, increase in sieve hole diameter is associated with a maxima. It is therefore advisable to avoid the hole diameter range around which irreversibility is high. It may be noted that this diameter range depends on the properties of the system components.

REFERENCES

1. J. L. Humphrey and A. F. Seibert, Separation technologies: an opportunity for energy savings, *Chem. Engng Prog.* **88**(3), 32–41 (1992).
2. A. Bejan, A study of entropy generation in the fundamental convective heat transfer, *ASME J. Heat Transfer* **101,** 718 (1979).
3. A. Bejan, Second law analysis in heat transfer. In *Advances in Heat Transfer* (Edited by J. P. Hartnett and T. F. Irvine, Jr.), Vol. 15, p. i (1982).
4. A. Bejan, The concept of irreversibility in heat exchanger design: counterflow exchanger of gas-to-gas applications, *ASME J. Heat Transfer* **99,** 374 (1977).
5. A. Bejan, General criterion for rating of heat exchanger performance, *Int. J. Heat Mass Transfer* **21,** 665 (1978).
6. P. J. Golem and T. A. Brzustowski, Second law analysis of thermal processes, *Trans. CSME* **4,** 219 (1977).
7. S. Sarangi and K. Chowdhury, On the generation of entropy in a counterflow heat exchanger, *Cryogenics* **22,** 63–65 (1988).
8. P. K. Nag and P. Mukherjee, Thermodynamic optimisation of convective heat transfer through a duct with constant wall temperature, *Int. J. Heat Mass Transfer* **30,** 401–405 (1987).
9. S. K. Som, A. K. Mitra and S. P. Sengupta, Second law analysis of spray evaporation, *J. Energy Resour. Technol.* **112**(2), 130–135 (1990).
10. J. F. and B. O. G. Schuler, Bubble formation at an orifice in viscous liquid, *Trans. Instn Chem. Engrs* **38,** 144 (1960).
11. A. Kupferberg and G. J. Jameson, Bubble formation at a submerged orifice above a gas chamber of finite volume, *Trans. Instn Chem. Engrs* **47,** T241–250 (1969).
12. A. Kupferberg and G. J. Jameson, Pressure fluctuations in a Bubbling Column with special reference to sieve plates, *Trans. Instn Chem. Engrs* **48,** T140–150 (1969).
13. R. D. La Nauze and I. J. Harris, On a model for the formation of gas bubbles at a single submerged orifice under constant pressure conditions. *Chem. Engng Sci.* 2102–2105 (1972).
14. O. E. Potter, Bubble formation under constant pressure conditions, *Chem. Engng Sci.* **24,** 1733–1736 (1969).
15. A. Satyanarayan, R. Kumar and N. R. Kuloor, Studies on bubble formation—II. Bubble formation under constant pressure conditions, *Chem. Engng Sci.* **29,** 749–761 (1969).
16. F. J. Zuiderweg, Sieve trays: a view of the state of art, *Chem. Engng Sci.* **37**(10), 1441–1464 (1982).
17. W. R. Marshall, Jr., *Atomosation and Spray Drying, Chem. Engng Prog. Monogr.* Ser. no. 2, Vol. 50, p. 87, AIChE Publications (1954).